Cell type-specific dynamics of prefrontal gamma synchrony during flexible behavior

Aarron J. Phensy[1,2], Lara L. Hagopian[1,2], Vikaas S. Sohal[1,2]

[1] Department of Psychiatry and Behavioral Sciences, San Francisco, CA 94143-0444
[2] Weill Institute for Neurosciences, Center for Integrative Neuroscience, and Kavli Institute for Fundamental Neuroscience, University of California, San Francisco, San Francisco, CA 94143-0444

Abstract

The prefrontal cortex (PFC) is required for many cognitive processes that are disrupted in conditions such as schizophrenia. The PFC is composed of neuronal networks which are organized by both local microcircuitry and inter-regional projections, within which precisely tuned neuronal activity generates appropriate cognitive responses. Parvalbumin-positive interneurons (PVI) play an integral role by synchronizing select networks to oscillations in the gamma frequency range (~30-100 Hz). Synchronized gamma oscillations seem to facilitate information transfer between neurons and across regions. In particular, our lab has previously shown that PVI-generated gamma oscillations in the left and right prefrontal cortices become synchronized during cognitive tasks and this synchronization is necessary for animals to learn rule shifts. Here, we examine how this synchrony propagates through prefrontal circuits using novel genetically encoded voltage indicators (GEVIs) to examine gamma oscillations in specific populations of deep layer projection neurons targeting either the mediodorsal thalamus (PFC-MD) or dorsal striatum (PFC-DS). We first designed a novel analysis which found that PVI exhibit inter-hemispheric gamma synchrony immediately (within seconds) following trial outcomes, during a specific subset of trials associated with the adoption of a new behavioral strategy. PFC-MD neurons did not exhibit gamma synchrony during these outcome periods, but did synchronize during the pre-decision period of the next trial. Furthermore, pre-decision gamma synchrony in PFC-MD neurons was dependent on PVI and did not occur in PFC-DS neurons. Together, our findings suggest that gamma synchrony is transmitted from PVI to PFC-MD neurons during rule shifts in a task-phase and cell type-specific manner to facilitate the updating of behavioral strategies.

Introduction

Cognitive deficits are a core symptom in schizophrenia that have a great impact on the quality of life of affected individuals[1,2]. Many of these deficits are attributed to neural circuit dysfunction within the dorsolateral prefrontal cortex[3] and between the prefrontal cortex and other regions such as the mediodorsal thalamus[4,5] and dorsal striatum[6,7]. Synchronized rhythmic neural activity (oscillations) between these regions is believed to reflect information flow across the brain. Of note, deficits in neural oscillations in the gamma frequency band (~30-100 Hz) are heavily documented in schizophrenia, including a reduction in evoked gamma oscillatory power during cognitive control tasks such as the Wisconsin Card Sorting Task (WCST)[3,8]. This loss of task-evoked gamma activity correlates with performance and is believed to reflect an inability of the PFC to appropriately process changes within the environment that signal a need to alter behavior. Parvalbumin-expressing GABAergic interneurons (PVI) comprise nearly half of all interneurons in the cortex and are believed to be a critical mediator of gamma oscillations in the brain[9]. Importantly, reductions in PVI function are one of the core pathologies associated with schizophrenia[10] and likely a major contributor to the altered gamma activity observed in individuals with schizophrenia. In animals, loss of PVI function in the prefrontal cortex (PFC) has extensively been studied in models used to study schizophrenia[11,12] and results in aberrant gamma

oscillatory activity[12,13] and reduced cognitive flexibility[14,15]. Recent work from our lab has identified that prefrontal PVI not only act as local generators of gamma oscillations, but also synchronize gamma activity across left and right prefrontal cortices as mice perform a task involving cognitive flexibility[16]. Importantly these studies identified that this gamma synchrony (γ-Synchrony) is *necessary* for mice to appropriately perform the task and that optogenetic enhancement of γ-Synchrony in PVI can rescue cognitive deficits in mutant mice with impaired PVI function[16]. These findings suggest that PVI-mediated γ-Synchrony may play an active role in propagating task-relevant information between brain regions. Importantly, PVI are known to enhance entrainment of deep layer projection neurons through a combination of feed-forward and feed-back inhibition[9,17] and may be responsible for promoting γ-Synchrony in these cells, thereby regulating inter-regional communication. Here, we propose that cross-hemispheric γ-Synchrony of prefrontal PVI can selectively promote entrainment of downstream projection neurons via gamma oscillations and enhance inter-hemispheric (left and right prefrontal cortices) γ-Synchrony within these populations.

Results

<u>Parvalbumin Interneurons (PVI) exhibit enhanced γ-Synchrony within seconds after trial outcomes when mice shift between goal-oriented strategies.</u> Our lab previously identified that PVI synchronize at gamma frequencies (30-50 Hz) across left and right prefrontal cortices during a rule-shift task – specifically following error trials [16], however whether this occurred immediately after the errors or later (e.g. in the inter-trial-interval period, or next trial) was not known. To further examine this phenomenon, we expressed the genetically encoded voltage indicator (GEVI) Ace-mNeon in prefrontal PVI (Fig 1A-B) and performed trans-membrane electrical measurements performed optically (TEMPO)[16,18] which allows for cell-specific recordings of voltage activity with fast kinetics (<1ms). In addition, we developed a novel analysis pipeline that enabled us to measure cross-hemispheric synchrony during behaviorally relevant epochs as brief as 1s (Fig 1C, Methods). Mice then performed a variant of the rule-shift task which has been used extensively in our lab[12] in which mice are presented with compound cues (2 modalities: odor + texture) and have to first establish a reward-association with a specific cue within a given modality (Initial Association; e.g. attend texture) and then shift this association to a different cue belonging to the previously ignored modality (Rule Shift; e.g. ignore texture, attend odor; Fig 1D-E). This shift across modalities is considered an extra-dimensional shift and requires a functioning PFC[19] and is dependent on PVI-activity[12]. Importantly, to enhance our ability to time-lock neural recordings to discrete behavioral moments we implemented a change to our previously-used behavioral protocol: instead of pre-baiting each correct bowl with a hidden food reward, when a mouse dug in their choice bowl, the experimenter either provided a reward with forceps (correct choice) or removed the correct bowl (error choice), thus giving precisely-timed and cued outcomes (Fig 1E). Interestingly, this extra step slightly increased trials to criterion and allowed us to examine learning across a larger spread of trials.

In this task, on 50% of trials, mice are presented with a cue-pairing in which the cue that was rewarded during the Initial Association and the cue that becomes rewarded during the Rule Shift cue are both located in the same bowl. Thus, mice would make a correct choice by following either rule. Conversely, on 50% of trials mice are presented with a cue-pairing in which the Initial Associated and Rule Shift cues are located in different bowls, such that selecting bowl containing the cue that was rewarded during the Initial Association would result in an error. Based on this we define two trial types: “Non-Conflict” trials, in which the Initial Association and Rule Shift cues are located in the same bowl, and “Conflict” trials in which these cues are located in different bowls (Fig 1D). Using these trial delineations, we were able to

identify a key period of behavioral transition which captured the time during which mice shift their behavioral strategy to choosing the cue which has newly become associated with reward during the Rule Shift. This period consists of the last two conflict trials which result in errors and first two conflict trials which result in correct outcomes (Fig 2A). Next, we measured γ-Synchrony within PVI across left and right prefrontal cortices by performing cross-correlational analysis on Ace-mNeon signals from each hemisphere which had been 'cleaned' (to remove artifacts) by subtracting a scaled version of the reference fluorophore signal. We then compared PVI γ-Synchrony from either the pre-decision (3 seconds leading up to mouse dig) or post-outcome (4 seconds following reward or bowl removal) periods across three behaviorally-defined trial types: 1) all Non-Conflict trials, 2) Conflict trials outside of the behavioral transition period ('Non-Transition Conflict trials'), and 3) Conflict trials within the behavioral transition period ('Transition Conflict trials'). Interestingly, PVI γ-Synchrony did not show significant differences between any of these trial types during the pre-decision period ($F_{(2,24)} = 2.0$, $p = 0.157$; Fig 2C). In contrast, when we examined PVI γ-Synchrony during the post-outcome period we found that there was a significant increase in PVI γ-Synchrony specifically during Transition Conflict trials ($F_{(2,24)} = 6.126$, $p = 0.007$; Fig 2D). In addition, we wanted to examine how PVI γ-Synchrony changed throughout behavior as mice encountered Conflict trials. Thus, we grouped all Conflict error trials (aligned across mice using the final conflict error as a reference point) and all Conflict correct trials (aligned across mice using the first conflict correct trial as a reference point) and measured how PVI γ-Synchrony changed within each group of trials (Fig 2E-F). When we examined PVI γ-Synchrony within the pre-decision period, we did not observe any fluctuations in PVI γ-Synchrony as behavior evolved (Fig 2E). However, in the post-outcome period, we observed a trend in which PVI γ-Synchrony is enhanced as animals enter the behavioral transition period and then subsides after the animal adapts to the new rule (Fig 2F). These findings are the first evidence showing that PVI quickly and robustly synchronize across hemispheres within seconds after outcomes during transient periods, specifically during periods in which animals are shifting strategies.

<u>γ-Synchrony emerges in PFC-MD, but not PFC-DS, neurons during the pre-decision period as mice shift to new strategies</u>

To enable flexible behaviors, the prefrontal cortex communicates with other regions known to be involved in cognitive functions. Two major projections from the PFC include the mediodorsal thalamus (MD) and the dorsal striatum (DS) which are both heavily implicated in supporting flexible behaviors[5,20,21]. Thus, we next wanted to examine if PVI proffer γ-Synchrony onto PFC neurons projecting to either of these regions (PFC-MD or PFC-DS). Importantly, these cell-types are intermingled within deep layers of the PFC, making it challenging for traditional electrophysiological methods to identify distinct roles for these two populations in behavioral flexibility. However, with the use of GEVIs we can examine oscillatory behavior specifically within each of these populations. Therefore, we specifically expressed Ace-mNeon within either population by injecting a retrograde Cre virus (CAV2-Cre) in either the MD or DS (Fig 3A), then examining γ-Synchrony during our rule shift task. We first examined PFC-MD γ-Synchrony across the same behaviorally defined trial types as we did with PVI. Surprisingly, though PVI exhibit a robust increase in γ-Synchrony within the post-outcome period of Transition Conflict trials, we did not observe an increase similar in synchrony within the PFC-MD neurons during the outcome period ($F_{(2,21)} = 2.291$, $p = 0.126$; Fig 3C). Instead, we observed an increase in PFC-MD γ-Synchrony specifically during the pre-decision period. There was a modest increase in PFC-MD γ-Synchrony on Non-Conflict trials ($F_{(2,21)} = 3.468$, $p = 0.050$). Because behavioral strategies are rapidly updated during the behavioral transition period, and during this period PVI exhibit markedly increased γ-Synchrony immediately

following Conflict trial outcomes, we wondered if this PVI γ-Synchrony might alter PFC-MD γ-Synchrony during the subsequent pre-decision period. Therefore, we examined PFC-MD γ-Synchrony during the pre-decision following each of our trial types ('t+1 pre-decision period'). Strikingly, we observed a pronounced increase in PFC-MD γ-Synchrony specifically during the pre-decision period immediately following Conflict trials during the behavioral transition ($F_{(2,21)} = 6.407$, $p = 0.007$, Fig 3C), thus revealing the modulation of PFC-MD activity related to decisions specifically as animals shift between strategies. Furthermore, when we examined γ-Synchrony in PFC-DS mice we did not observe any increases in γ-Synchrony between any of the trial types during pre-decision ($F_{(2,27)} = 1.233$, $p = 0.307$), post-outcome ($F_{(2,27)} = 1.137$, $p = 0.336$), or t+1 pre-decision periods ($F_{(2,27)} = 0.455$, $p = 0.639$; Fig 3D). This was highly surprising, because it suggests that γ-Synchrony does not engage all cell types within a local microcircuit (e.g. layer 5-6 of PFC), but rather manifests in specific cell types, distinguished by their projection targets.

PVI are necessary for γ-Synchrony dynamics in PFC-MD neurons

PVI have been shown to be critical for pyramidal neuron entrainment to gamma oscillations [9]. Therefore, we wondered if PVI were necessary for the emergence of γ-Synchrony that we observed in PFC-MD neurons. To test this, we once again expressed Ace-mNeon in MD-projecting neurons in the PFC, but additionally injected a Flp-dependent virus to express the inhibitory opsin, halorhodopsin, (fDIO-NpHR-BFP) into the PFC of both PV-Flp$^{+/-}$ transgenic mice and wild-type controls (Fig 4A-B). We then performed rule shifting over two days. On Day 1, animals performed the rule shift task as normal while we recorded γ-Synchrony in PFC-MD neurons. On Day 2 , mice performed the task again (using different rules than on Day 1), however, this time we activated NpHR via delivery of 638nm laser stimulation during the rule shift portion of the task (Fig 4C). Importantly, as previously reported, optogenetic inhibition of prefrontal PVI resulted in reduced performance, i.e., PV-Flp$^{+/-}$ mice required significantly more trials to learn the rule shift compared to wild-type controls (simple main effect of genotype: $F_{(1,15)} = 5.116$, $p = 0.04$,0 Fig 4D). PV-Flp$^{+/-}$ mice also exhibited more perseverative behavior, evidenced by significant increases in both correct outcomes on Non-Conflict trials and error outcomes on Conflict trials (interaction trial type x task day: $F_{(3,54)} = 9.614$, $p < 0.001$; simple main effect of trial type: $F_{(1.663,29.93)} = 15.9$, $p < 0.001$; Fig 4E).

We then again examined PFC-MD γ-Synchrony during the t+1 pre-decision period in both wild-type and PV-Flp$^{+/-}$ mice across trial types on Day 1. As before, we observed a significant increase in the PFC-MD γ-Synchrony specific to Transition Conflict trials in both wild-type ($F_{(2,15)} = 6.330$, $p = 0.010$, Fig 4F) and PV-Flp$^{+/-}$ mice ($F_{(2,27)} = 10.10$, $p < 0.001$, Fig 4G). Next, we examined the effect of delivering 638nm stimulation to inhibit PVI during the rule shift on Day 2. In wild-type mice, the increase in PFC-MD γ-Synchrony was still observed ($F_{(2,15)} = 8.085$, $p = 0.004$, Fig 4H) demonstrating that this effect is stable across task days. However, when PVI were inhibited in PV-Flp$^{+/-}$ mice, this increase was abolished, i.e., there was no change in PFC-MD γ-Synchrony across trial types ($F_{(2,27)} = 0.889$, $p = 0.4229$, Fig 4I). This demonstrates that even though γ-Synchrony increases in PVI and PFC-MD neurons at different task phases, γ-Synchrony in PFC-MD neurons still depends on PVI activity.

Discussion

Here we demonstrate that PVI-mediated γ-Synchrony appears on the timescales of seconds and is tightly coupled to behavioral events. We first show that γ-Synchrony emerges in PVI rapidly following outcomes on trials which involve a decision conflict between the old and new rules, specifically when mice are in the process of adopting a new strategy (Fig 2). This was a surprising result as previous work from our lab has primarily seen increases in γ-Synchrony following error trials[16,22]. However, this difference is likely

due to the modified task used here. In particular, in our original version of the task (in which mice find food rewards hidden within each bowl), mice typically learn rule shifts rapidly, after making just 2-3 errors. Almost all of these are perseverative errors, meaning they occur on Conflict trials. Thus, in our earlier studies, identifying periods following rule shift errors will yield mainly Conflict trials during behavioral transition. This corresponds to the same type of trials for which this study observed increased γ-Synchrony during the post-outcome period. Furthermore, this study also examined γ-Synchrony on relatively short timescales – thus it may be that error outcomes lead to a more persistent elevation in γ-Synchrony (e.g., lasting into the inter-trial interval) as compared to correct outcomes. Regardless, elevations in PVI γ-Synchrony in all studies preceded shifts in behavior and are consistent with a framework in which prefrontal PVI γ-Synchrony is necessary to enable cognitive flexibility.

We next demonstrate that γ-Synchrony also emerges in PFC-MD neurons specifically within the pre-decision period as animals shift to a new strategy (Fig 3). Notably this did not occur in another population projecting to the dorsal striatum (PFC-DS). These findings are remarkable for a few reasons. First, the fact that γ-Synchrony emerges in PFC-MD neurons and not PFC-DS neurons (even though they are both located in the same cortical layers) suggests that γ-Synchrony is not a generalized phenomenon reflecting synchronized activity across prefrontal microcircuits, but rather reflects select activation within specific neuronal populations that likely convey information out of the PFC to particular downstream targets. Second, the fact that γ-Synchrony emerges in PFC-MD following trials in which we observed γ-Synchrony in PVI hints at a potential mechanism in which PVI γ-Synchrony during the post-outcome period of one trial may result in the emergence of γ-Synchrony in PFC-MD neurons on the pre-decision period of the following trial. Indeed, we found that PFC-MD γ-Synchrony required activity of PFC-PVI neurons (Fig 4), supporting this concept. Further work will need to identify causal relationships between γ-Synchrony dynamics in PVI and PFC-MD neurons. Finally, these findings highlight the power and importance of using genetically encoded voltage indicators to identify unique oscillatory properties of different cell populations that are co-localized within the same region.

In summary, these findings demonstrate that PVI have the ability to coordinate information flow across cell types and across regions, further stressing their importance for facilitating inter-regional communication across the brain. Further, we demonstrate a role for γ-Synchrony in PFC-MD neurons that is related to updating choice behavior during rule shifts. Future work could identify how enhancing synchrony in this circuit, or between the PFC and MD, might facilitate the ability to change outdated behaviors and thus may have clinical relevance for designing therapeutics aimed to enhance cognitive functioning in schizophrenia or other psychiatric conditions.

Methods

<u>Animals and Housing Conditions</u>

Animals of both male and female sexes were used for all experiments. Mice were normally group housed in a normal light / dark cycle with ad libitum access to food. For rule shift behaviors animals were moved to a reverse light / dark schedule and singly housed for the duration of behavior. During this time animals were food restricted (as described below) over the course of ~ 1 week to 85% of baseline weight.

For experiments examining GEVI expression in PVI, animals of PV-Cre (Jax; 017320) line were crossed with Ai14 (Jax; 007914) to generate PV-Cre$^{+/-}$ / Ai14$^{+/-}$ mice enabling expression of ACE-mNeon and TdTomato in prefrontal PVI. For experiments examining GEVI expression in PFC-MD or PFC-DS neurons,

Ai14 mice were used for all experiments. For experiments combining GEVI expression in PFC-MD neurons with fDIO-NpHR3.0-BFP expression in prefrontal PVI, animals of the PV-Flp (Jax; 022730) line were crossed with Ai14 to generate PV-Flp$^{+/-}$ / Ai14$^{+/-}$ mice enabling expression of ACE-mNeon and TdTomato in PFC-MD neurons and NpHR3.0-BFP in prefrontal PVI. PV-Flp$^{-/-}$ / Ai14$^{+/-}$ from the same litters were used as wild-type controls.

Rule Shift Behavior

See figure 1D-E. Methods are adapted from previous work[16]. In short, mice are first food restricted to 85% of baseline weight. Mice then undergo habituation where they are trained to dig in one of two bowls containing complex cues each consisting of an odor and texture modality. The bowl pairs are organized into 2 presentations: 1. Litter + Coriander and Sand + Garlic or 2. Litter + Galic and Sand + Coriander. During habituation cues are evenly rewarded and no cue-reward association is formed. Mice learn to do this relatively fast, and habituation is completed over the course of 10 presentations (trials). On the next day mice perform the task which is broken into two parts: Initial Association (IA) – mice are trained to attend a specific modality and discriminate between the two cues to receive a reward (e.g. IA Rule: Sand: mice must dig in either Sand + Garlic or Sand + Coriander bowls depending on presentation). If mice dig in the correct bowl, a reward (peanut butter chip) is delivered to the mouse using forceps and then they are placed in a holding cage for ~30 seconds while the next trial is prepared. If mice dig in the incorrect bowl, then the experimenter removes the correct bowl (to signal an error) and mice are placed in a holding cage for ~90 seconds. After animals achieve a behavioral criterion of 8/10 correct choices in a row, animals directly begin the next portion: Rule Shift. During the Rule Shift, the reward-cue pairing is shifted across modalities (e.g. IA Rule: Sand -> RS Rule: Garlic: mice must dig in either Sand + Garlic or Litter + Garlic). This shift is uncued and requires animals to ignore the previous rule's modality while attending the new modality which is considered an extradimensional shift. Note that 50% of the time an animal can use the IA rule and still get a correct choice (e.g. IA Rule: Sand -> RS Rule: Garlic, Sand + Garlic choice), these trials are considered 'Non-Conflict' trials, whereas the other trials (e.g. requiring Litter + Garlic choice) are considered 'Conflict' trials since animals must actively ignore the IA rule. Correct and error trials are handled the same as in IA and animals continue the behavior until they once more reach a criterion of 8/10 trials.

Stereotactic Surgeries

Male and female mice were anaesthetized using isoflurane (2.5% induction, 1.2–1.5% maintenance, in 95% oxygen) and placed in a stereotaxic frame (David Kopf Instruments). Body temperature was maintained using a heating pad. An incision was made to expose the skull for stereotaxic alignment using bregma and lambda as vertical references. The scalp and periosteum were removed from the dorsal surface of the skull and scored with a scalpel to improve implant adhesion. Viruses were infused at 100–150 nl min−1 through a 35-gauge, beveled injection needle (World Precision Instruments) using a microsyringe pump (World Precision Instruments, UMP3 UltraMicroPump). After infusion, the needle was kept at the injection site for 5–10 min and then slowly withdrawn. After surgery, mice were allowed to recover until ambulatory on a heated pad, then returned to their home cage. For all experiments, we waited at least 5 weeks to allow for virus expression prior to beginning behavioral experiments.

For experiments investigating γ-Synchrony in prefrontal PVI, PV-Cre$^{+/-}$ / Ai14$^{+/-}$ mice were injected bilaterally into the mPFC (+1.7 AP, +/-0.3ML, three depths: -2.5, -2.25, -2 DV) with 200nL (per depth) of AAV1-CAG-DIO-Ace2N-4AA-mNeon (Virovek). After injection of virus, two mono fiber-optic cannulas

(Doric Lenses; MFC_400/430-0.48_2.8mm_ZF1.25_FLT) were lowered into the left and right prefrontal cortices (+1.7 AP, +/- 0.76ML, -2.13DV) at a 12-degree angle.

For experiments investigating γ-Synchrony in deep layer PFC neurons targeting either the MD or DS, Ai14$^{+/-}$ mice were injected bilaterally into the mPFC (+1.7 AP, +/-0.5ML, three depths: -2.5, -2.25, -2 DV) with 200nL (per depth) of AAV1-CAG-DIO-Ace2N-4AA-mNeon (Virovek). In addition, mice were injected bilaterally into either the mediodorsal thalamus (-1.7 AP, +/-0.35ML, -3.5DV) or dorsal striatum (+0.9 AP, +/-1.0ML, -3.0 DV) with 350nL (per site) with CAV2-Cre (Plateforme de Vectorologie de Montpellier). After injection of virus, two mono fiber-optic cannulas (Doric Lenses; MFC_400/430-0.48_2.8mm_ZF1.25_FLT) were lowered into the left and right prefrontal cortices (+1.7 AP, +/- 0.8ML, -2.2DV) at a 12-degree angle.

For experiments combining the investigation of γ-Synchrony in MD-projecting neurons with inhibition of prefrontal PVI, PV-Flp$^{+/-}$ / Ai14$^{+/-}$ mice were injected bilaterally into the mPFC (+1.7 AP, +/-0.5ML, three depths: -2.5, -2.25, -2 DV) with 250nL (per step) of a 1:1 ratio of AAV1-CAG-DIO-Ace2N-4AA-mNeon (Virovek) and AAV8-nEF-Coff/Fon-NpHR3.3-BFP (Virovek). In addition, mice were injected bilaterally into the mediodorsal thalamus (-1.7 AP, +/-0.35ML, -3.5DV) with 350nL (per site) with CAV2-Cre (Plateforme de Vectorologie de Montpellier). After injection of virus, two mono fiber-optic cannulas (Doric Lenses; MFC_400/430-0.48_2.8mm_ZF1.25_FLT) were lowered into the left and right prefrontal cortices (+1.7 AP, +/- 0.8ML, -2.2DV) at a 12-degree angle.

Recording of GEVI Activity and Analysis

Methods are described in detail in previous work[22] but are described in brief here. Per recording site, activation of ACE-mNeon and tdTomato fluorophore was accomplished using two fiber-coupled LEDS (Thorlabs; M490Fr and M565F3) controlled by an LED Driver (Thorlabs; DC4104) and each LED was modulated by a sinusoidal signal provided by a lock-in amplifier (Stanford Research Systems; SR860) at a specific frequency to allow for demodulation of each signal. Both LEDs were fed into a 'mini-cube' (Doric Lenses, FMC5_E1(460-490)_F1(500-540)_E2(555-570)_F2(580-600)_S) and then transmitted into the animal through an mono fiber-optic patch cord (Doric Lenses, MFP_400/430/1100-0.48_2m_FC-ZF1.25) attached to the mono fiber-optic cannula implanted on the animal during surgery. GEVI emissions were captured through the same 'mini-cube' and fed into a photoreceiver (FEMTO OE-200-SI-FC) which sends the resulting signal back to the lock-in amplifier. All four signals are then demodulated and then digitized by a multichannel real-time signal processor (Tucker-Davis Technologies, RX-8). The commercial software Synapse (Tucker-Davis Technologies) was used for data acquisition.

For experiments that combined GEVI recordings with optogenetic inhibition of PVI, the system was the same as described above, however a different 'mini-cube' was used that had an additional opto-port (Doric Lenses, FMC6_E1(460-490)_F1(500-540)_E2(555-570)_F2(580-600)_O(628-642)_S) which was connected to a 638nm laser (Doric Lenses).

To quantify cross-hemispheric γ-Synchrony in cell populations at resolutions up to 250ms we generated a novel form of analysis. After data acquisition, data was converted from the proprietary Tucker-Davis Technologies tank format into a MATLAB structure using the SEV2Mat file (Tucker-Davis Technologies). We then extracted all four signals (Left Hemisphere: ACE-mNeon, tdTomato; Right Hemisphere: ACE-mNeon, tdTomato). We then performed 'signal cleaning' by performing linear regression between ACE-mNeon and tdTomato signals and subtracting the shared noise from the ACE-mNeon signal, thus

resulting in a 'clean' signal that is free of shared, non-voltage, noise. Signals were then filtered within the frequency of interest (30-50hz for gamma). Finally, we took the cross-correlation between the left and right hemisphere's cleaned signals across the full session in 250ms bins thus generating a metric of γ-Synchrony across the entire session. In addition, we included a phase shift between -180 to 180 degrees and identified the phase with peak correlation as that time-point's 'preferred' phase. Signals which had a 'preferred' phase between -45 to 45 degrees were considered 'In-Phase' and were utilized for further analysis. For z-scored data, a baseline period of 10minutes prior to the start of behavior was used to normalize data.

Histological Tissue Validation

Following experiments animals were anesthetized with an i.p. injection of Euthasol and transcardially perfused with 30 ml of ice-cold 0.01 M PBS followed by 30 ml of ice-cold 4% paraformaldehyde in PBS. Brains were extracted and stored in 4% paraformaldehyde for 24 h at 4 °C before being stored in PBS. Slices 70–100 µm thick were obtained on a Leica VT100S and mounted on slides. All imaging was performed on an Olympus MVX10, Keyence BZ-X All-in-One Fluorescence Microscope, or Nikon Crest LFOV Spinning Disk/ C2 Confocal. All mice were verified to have virus-driven expression and optical fibers located in the mPFC.

References

1. Green, M. F., Llerena, K. & Kern, R. S. The "Right Stuff" Revisited: What Have We Learned About the Determinants of Daily Functioning in Schizophrenia?: Fig. 1. *SCHBUL* **41**, 781–785 (2015).
2. Zhu, C., Kwok, N. T., Chan, T. C., Chan, G. H. & So, S. H. Inflexibility in Reasoning: Comparisons of Cognitive Flexibility, Explanatory Flexibility, and Belief Flexibility Between Schizophrenia and Major Depressive Disorder. *Front. Psychiatry* **11**, 609569 (2021).
3. Boudewyn, M. A. & Carter, C. S. Evolving Concepts in Brain Oscillations and Cognitive Control in Schizophrenia. *Biological Psychiatry* **84**, 632–633 (2018).
4. Collins, D. P., Anastasiades, P. G., Marlin, J. J. & Carter, A. G. Reciprocal Circuits Linking the Prefrontal Cortex with Dorsal and Ventral Thalamic Nuclei. *Neuron* **98**, 366-379.e4 (2018).
5. Parnaudeau, S., Bolkan, S. S. & Kellendonk, C. The Mediodorsal Thalamus: An Essential Partner of the Prefrontal Cortex for Cognition. *Biological Psychiatry* **83**, 648–656 (2018).
6. Fornito, A. *et al.* Functional Dysconnectivity of Corticostriatal Circuitry as a Risk Phenotype for Psychosis. *JAMA Psychiatry* **70**, 1143 (2013).
7. Morris, R. W., Quail, S., Griffiths, K. R., Green, M. J. & Balleine, B. W. Corticostriatal Control of Goal-Directed Action Is Impaired in Schizophrenia. *Biological Psychiatry* **77**, 187–195 (2015).
8. Boudewyn, M. A., Scangos, K., Ranganath, C. & Carter, C. S. Using prefrontal transcranial direct current stimulation (tDCS) to enhance proactive cognitive control in schizophrenia. *Neuropsychopharmacol.* **45**, 1877–1883 (2020).
9. Sohal, V. S., Zhang, F., Yizhar, O. & Deisseroth, K. Parvalbumin neurons and gamma rhythms enhance cortical circuit performance. *Nature* **459**, 698–702 (2009).
10. Lewis, D. A., Curley, A. A., Glausier, J. R. & Volk, D. W. Cortical parvalbumin interneurons and cognitive dysfunction in schizophrenia. *Trends in Neurosciences* **35**, 57–67 (2012).
11. Lodge, D. J., Behrens, M. M. & Grace, A. A. A Loss of Parvalbumin-Containing Interneurons Is Associated with Diminished Oscillatory Activity in an Animal Model of Schizophrenia. *Journal of Neuroscience* **29**, 2344–2354 (2009).
12. Cho, K. K. A. *et al.* Gamma Rhythms Link Prefrontal Interneuron Dysfunction with Cognitive Inflexibility in Dlx5/6+/− Mice. *Neuron* **85**, 1332–1343 (2015).

13. Kujala, J. *et al.* Gamma oscillations in V1 are correlated with GABAA receptor density: A multi-modal MEG and Flumazenil-PET study. *Sci Rep* **5**, 16347 (2015).
14. Ferguson, B. R. & Gao, W.-J. PV Interneurons: Critical Regulators of E/I Balance for Prefrontal Cortex-Dependent Behavior and Psychiatric Disorders. *Front. Neural Circuits* **12**, 37 (2018).
15. Murray, A. J. *et al.* Parvalbumin-positive interneurons of the prefrontal cortex support working memory and cognitive flexibility. *Sci Rep* **5**, 16778 (2015).
16. Cho, K. K. A. *et al.* Cross-hemispheric gamma synchrony between prefrontal parvalbumin interneurons supports behavioral adaptation during rule shift learning. *Nat Neurosci* **23**, 892–902 (2020).
17. Spellman, T., Svei, M., Kaminsky, J., Manzano-Nieves, G. & Liston, C. Prefrontal deep projection neurons enable cognitive flexibility via persistent feedback monitoring. *Cell* **184**, 2750-2766.e17 (2021).
18. Marshall, J. D. *et al.* Cell-Type-Specific Optical Recording of Membrane Voltage Dynamics in Freely Moving Mice. *Cell* **167**, 1650-1662.e15 (2016).
19. Bissonette, G. B., Powell, E. M. & Roesch, M. R. Neural structures underlying set-shifting: Roles of medial prefrontal cortex and anterior cingulate cortex. *Behavioural Brain Research* **250**, 91–101 (2013).
20. Balleine, B. W., Delgado, M. R. & Hikosaka, O. The Role of the Dorsal Striatum in Reward and Decision-Making. *Journal of Neuroscience* **27**, 8161–8165 (2007).
21. Griffiths, B. J. *et al.* Rhythmic interactions between the mediodorsal thalamus and prefrontal cortex precede human visual perception. *Nat Commun* **13**, 3736 (2022).
22. Cho, K. K. A., Shi, J., Phensy, A. J., Turner, M. L. & Sohal, V. S. Long-range inhibition synchronizes and updates prefrontal task activity. *Nature* **617**, 548–554 (2023).

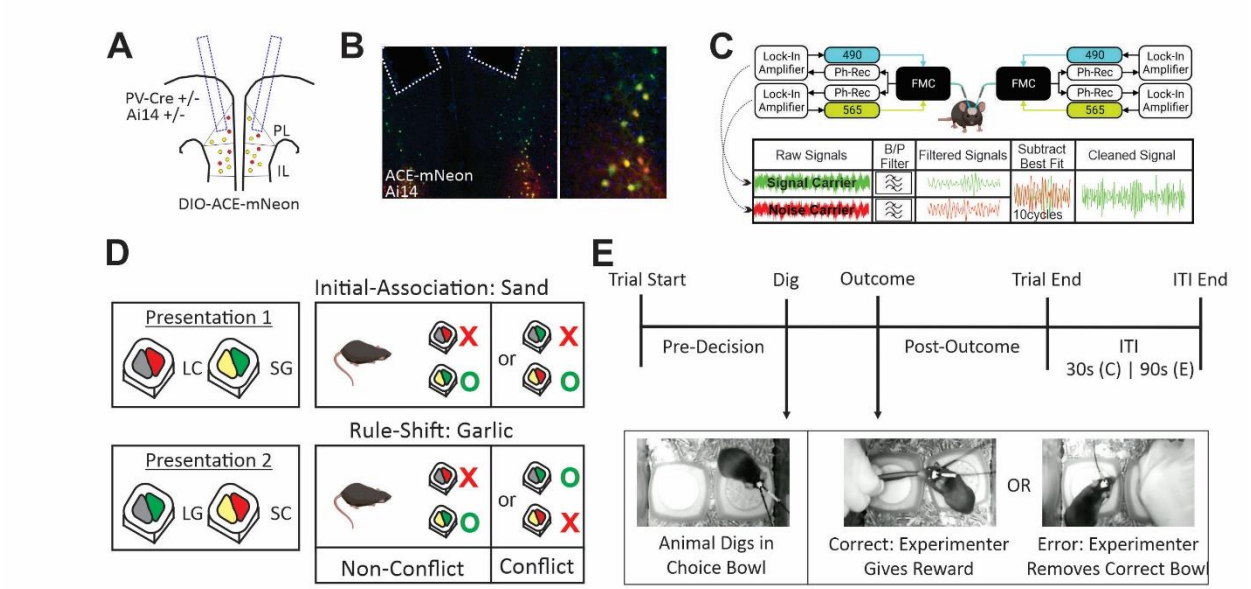

Figure 1. Experimental procedures for Genetically Encoded Voltage Indicators (GEVIs) and Rule Shift Behavior. A. Schematic demonstrating targeting strategy to express DIO-Ace-mNeon in PVI in the prefrontal cortex of PV-Cre$^{+/-}$; Ai14$^{+/-}$ mice. Bilateral implants designated as dotted lines. B. Representative image showing Ace-mNeon expression (green) and Ai14 (red) and co-localization (yellow). Dotted lines highlight implant position. C. Hardware configuration (top) utilizing 4 lock-in amplifiers to record Ace-mNeon (green) and tdTomato (red) signals from each hemisphere and analysis method (below) which subtracts a scaled version of the reference fluorophore (tdTomato) signal from the Ace-mNeon signal, to correct for artifacts and obtain a 'cleaned' voltage signal. D. Cartoon schematic of the rule shifting task. On each trial mice are presented with two bowls, each of which has a different odor (Coriander - 'C', or Garlic - 'G') and textured digging media (Litter - 'L', or Sand - 'S'). The odor-texture pairs vary from trial to trial. During the initial association the bowl containing one cue (here Sand) is consistently rewarded. Then, during the rule shift the rewarded cue shifts to a cue from the other modality (here Garlic). During the rule shift, on some trials the Initial Association cue and Rule Shift cues will be in the same bowl ('Non-conflict') while on the other trials they are located in different bowls ('Conflict'). E. Timeline of each trial. The 'Pre-Decision' period encompasses the time from the 'Trial Start' to when the mouse signifies a choice by digging in one bowl ('Dig'). The Outcome period is when the experimenter either delivers a reward (if the mouse digs in the correct bowl) or removes the non-chosen bowl (if the mouse digs in the incorrect bowl). The trial ends when the mouse is removed to a holding cage where it remains for the inter-trial interval (ITI) which is 30s following correct choices and 90s following errors.

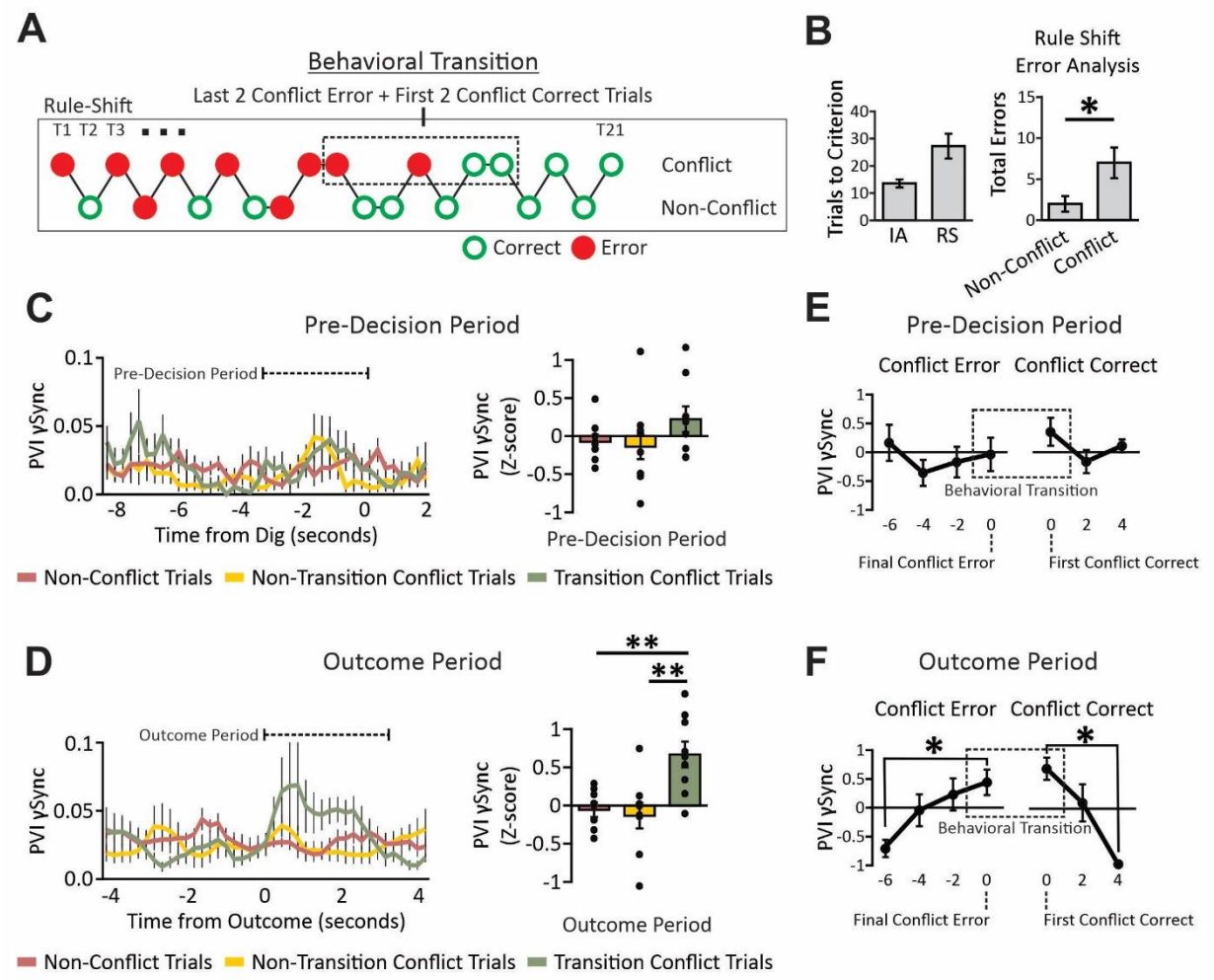

Figure 2. PVI exhibit γ-Synchrony following conflict trials during transitions to a new behavioral strategy. A. Schematic illustrating the 'Behavioral Transition' period which is defined as spanning the trials from the last 2 conflict errors to the first 2 correct conflict trials during the rule-shift portion of the task (dotted box). B. Number of trials to criterion for both the initial association (IA) and rule shift (RS) (left) and trial-type breakdown for rule shift errors (right). During rule shifts, mice make the bulk of the errors on conflict trials rather than on non-conflict trials. C. PVI γ-Synchrony for the pre-decision period for three trial types: all non-conflict trials, conflict trials existing outside of behavioral transition, and conflict trials during behavioral transition. Displayed as a trace time-locked to the time at which the animal digs in the chosen bowl (left) and averaged over the defined pre-decision period (right). D. Similar to C, however time-locked to the outcome (either the delivery of reward for correct choices or bowl removal for errors). PVI exhibit a significant increase in γ-Synchrony in the outcome period specifically during behavioral transitions. E. Average PVI γ-Synchrony as a function of trial number related to the final conflict error (left) or first correct conflict trial (right). There is no apparent change in pre-decision PVI γ-Synchrony during the transition to a new behavioral strategy. F. PVI exhibit a trend for an increase in γ-Synchrony on the last 2 conflict errors (left) and the first 2 conflict correct trials (right) which corresponds to the behavioral transition period. PVI γ-Synchrony is lower on trials preceding and following this behavioral transition period.

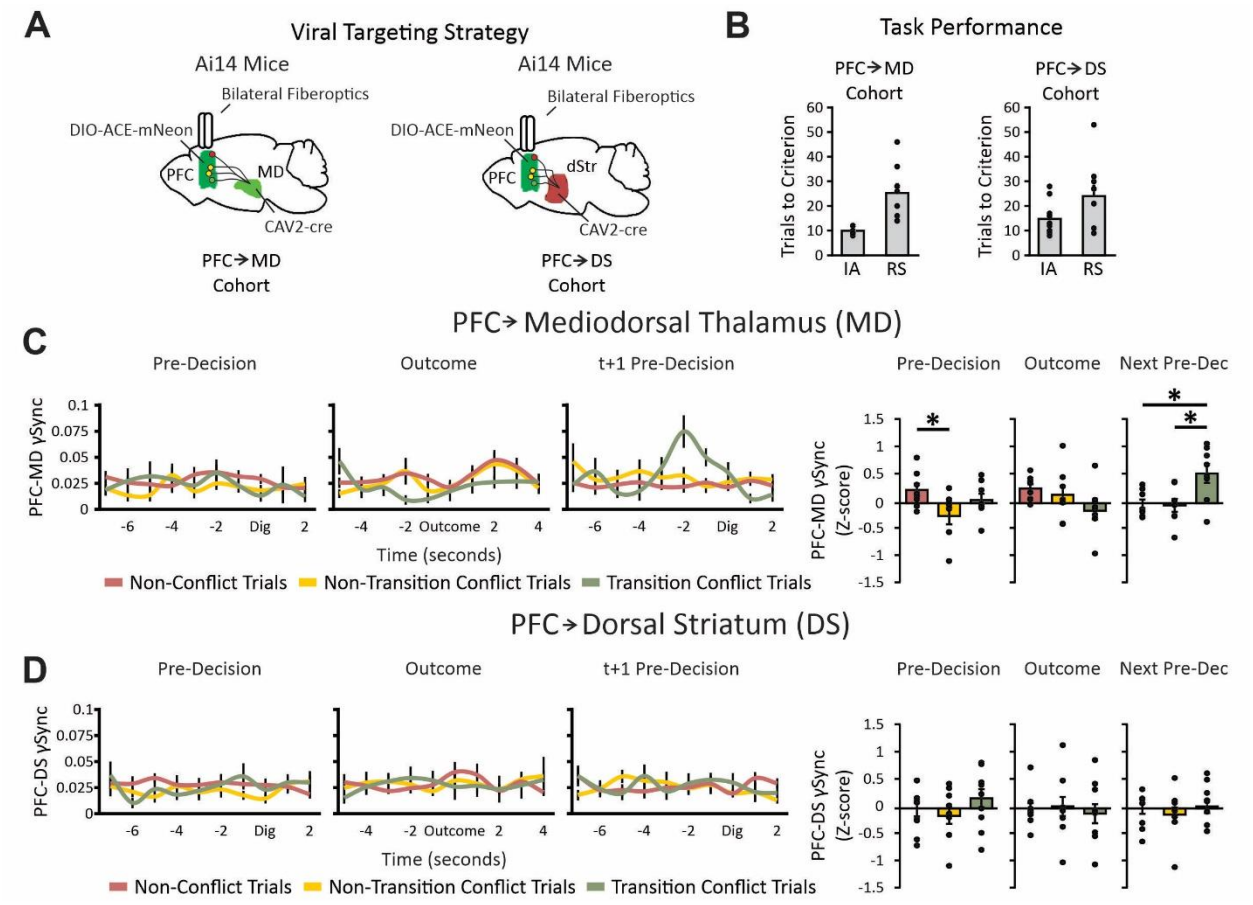

Figure 3. γ-Synchrony during rule shifts manifests in a cell type-specific manner. A. Viral targeting strategy to examine γ-Synchrony in prefrontal neurons projecting to either the mediodorsal thalamus (PFC-MD, left) or dorsal striatum (PFC-DS, right). B. Task performance for learning of the initial association (IA) and rule shift (RS) for both PFC-MD cohorts (left) and PFC-DS cohorts (right). C. Traces of γ-Synchrony for non-conflict, non-transition conflict, and transition conflict trials across three different periods: the pre-decision period of the current trial, outcome period of the current trial, and the pre-decision period of the following (t+1) trial (left). γ-Synchrony averaged over each respective period and (z-scored relative to the pre-task baseline period) (right). PFC-MD neurons exhibit different γ-Synchrony dynamics than PVI. There is a significant increase in γ-Synchrony during the pre-decision period of non-conflict trials. There is no significant change during the outcome period. There is also a significant increase in PFC-MD γ-Synchrony during the pre-decision period of trials which follow conflict trials (t+1) during the behavioral transition. D. Same as C, but for the PFC-DS cohorts. In contrast to both PVI and PFC-MD cohorts, there were not significant increase in γ-Synchrony during pre-decision, outcome, or t+1 pre-decision periods.

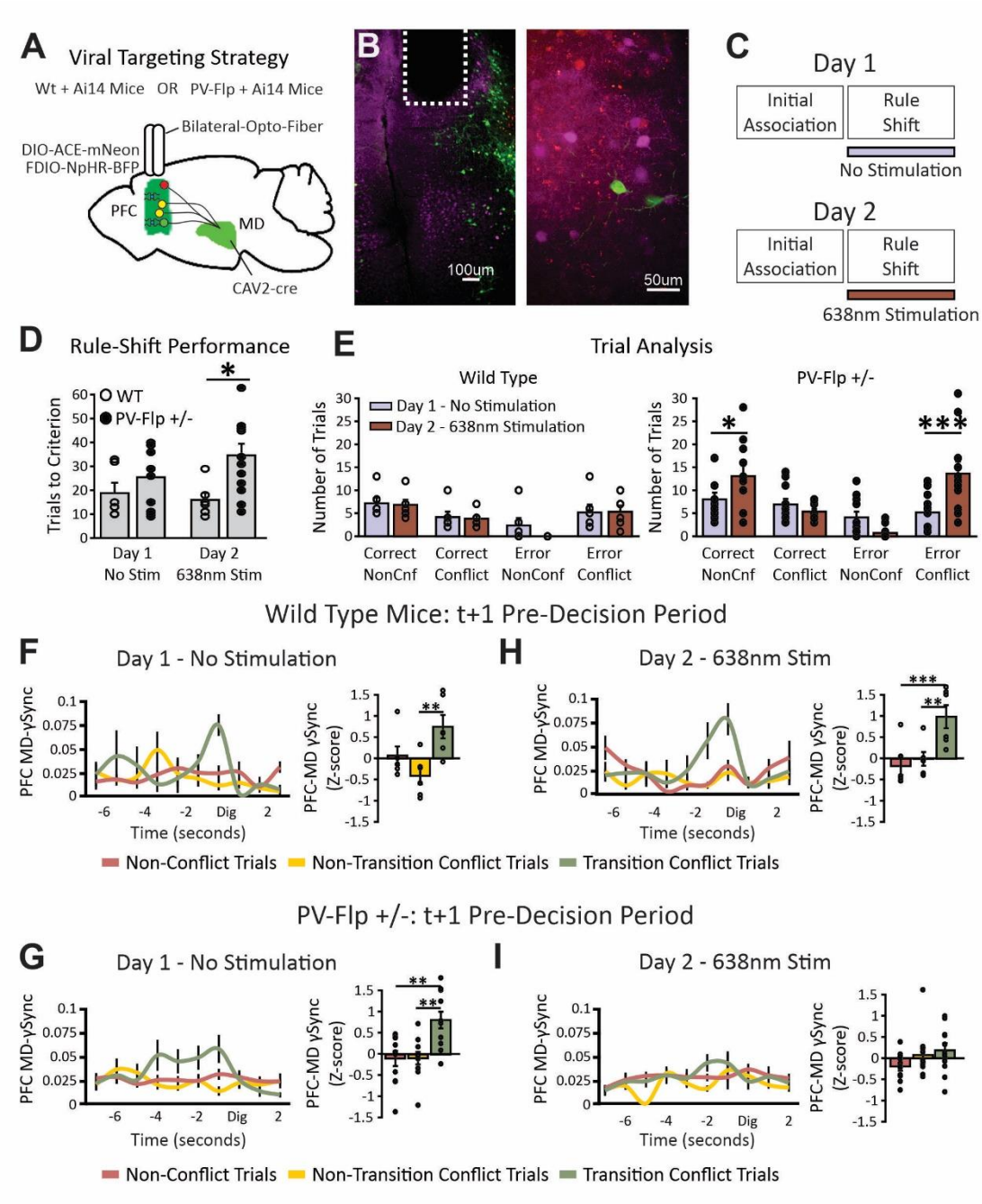

Figure 4. PVI are necessary for γ-Synchrony dynamics observed in PFC-MD neurons. A. Viral targeting strategy to inhibit prefrontal PVI with fDIO-NpHR-BFP while recording γ-Synchrony in PFC-MD neurons. B. Representative image of expression of Ace-mNeon (green), TdTomato (red), colocalization (yellow), and NpHR (purple). C. Stimulation strategy. Animals are run across 2 days. On Day 1, mice perform the rule shift task as normal without stimulation. On Day 2, PVI are inhibited through activation of NpHR with 638nm laser stimulation – specifically during the rule shift period. D. Rule shift performance across stimulation days for PV-Flp$^{+/-}$ mice and wild-type controls. PV-Flp$^{+/-}$ mice perform significantly worse on Day 2 compared to controls. E. Trial analysis for the rule shift portion of the task for both wild type (left)

and PV-Flp$^{+/-}$ mice (right). Inhibition of PVI results in a significant increase in both non-conflict correct trials and conflict error trials – both of which reflect perseverative behavior. F-G. Wild type (F) and PV-Flp$^{+/-}$ (G) mice exhibit an increase in PFC-MD γ-Synchrony in the t+1 pre-decision period specifically during behavioral transitions on Day 1. H. Wild type mice continue to exhibit an increase in PFC-MD γ-Synchrony in the t+1 pre-decision period on Day 2. I. However this is abolished in PV-Flp$^{+/-}$ mice which received inhibition of PVI (638nm stimulation).